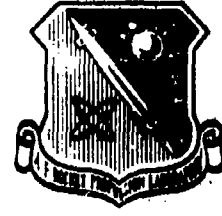


2

AFRPL-TR-81-80



**QUICK-LOOK STRUCTURAL ANALYSIS TECHNIQUES
FOR SOLID ROCKET PROPELLANT GRAINS**

Author: Russell A. Leighton

May 1982

Special Report for the period January 1981 to June 1981

APPROVED FOR PUBLIC RELEASE; DISTRIBUTION UNLIMITED

The AFRPL Technical Services Office has reviewed this report, and it is releasable to the National Technical Information Service, where it will be available to the general public, including foreign nationals.

**AIR FORCE ROCKET PROPULSION LABORATORY
DIRECTOR OF SCIENCE AND TECHNOLOGY
AIR FORCE SYSTEMS COMMAND
EDWARDS AFB, CALIFORNIA 93523**

**DTIC
ELECTE
OCT 04 1982
S D
E**

82 10 04 179

AD A119841

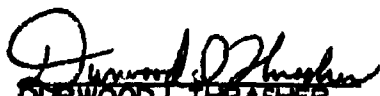
ALL INFORMATION CONTAINED HEREIN IS UNCLASSIFIED

NOTICES

When U.S. Government drawings, specifications, or other data are used for any purpose other than a definitely related Government procurement operation, the fact that the Government may have formulated, furnished, or in any way supplied the said drawings, specifications, or other data, is not to be regarded by implication or otherwise, or in any manner licensing the holder or any other person or corporation, or conveying any rights or permission to manufacture, use or sell any patented invention that may be related thereto.

FOREWORD

This Technical Report was prepared by the Mechanical Behavior and Aging Section (MKPB) of the Air Force Rocket Propulsion Laboratory under Job Order No. 573013NB. The principal author is Russell A. Leighton, who is employed under the California Polytechnic State University Cooperative Education Program. Mr Leighton worked under the guidance of Durwood Thrasher, the Senior Project Manager.


DURWOOD I. THRASHER
Project Manager


R. JOHN MOSS, Capt, USAF
Chief, Mechanical Behavior and
Aging Section

FOR THE DIRECTOR


CHARLES B. COOKE
Director, Solid Rocket Division

UNCLASSIFIED

SECURITY CLASSIFICATION OF THIS PAGE (When Data Entered)

REPORT DOCUMENTATION PAGE		READ INSTRUCTIONS BEFORE COMPLETING FORM
1. REPORT NUMBER AFRPL-TR-81-80	2. GOVT ACCESSION NO. All 9841	3. RECIPIENT'S CATALOG NUMBER
4. TITLE (and Subtitle) Quick-Look Structural Analysis Techniques for Solid Rocket Propellant Grains	5. TYPE OF REPORT & PERIOD COVERED Special Report	
	6. PERFORMING ORG. REPORT NUMBER	
7. AUTHOR(s) Russell A. Leighton	8. CONTRACT OR GRANT NUMBER(s)	
9. PERFORMING ORGANIZATION NAME AND ADDRESS Air Force Rocket Propulsion Laboratory/MKPB Edwards AFB CA 93523	10. PROGRAM ELEMENT, PROJECT, TASK AREA & WORK UNIT NUMBERS JON: 573013NB	
11. CONTROLLING OFFICE NAME AND ADDRESS	12. REPORT DATE May 1982	
	13. NUMBER OF PAGES 48	
14. MONITORING AGENCY NAME & ADDRESS (if different from Controlling Office)	15. SECURITY CLASS. (of this report) Unclassified	
	15a. DECLASSIFICATION/DOWNGRADING SCHEDULE NA	
16. DISTRIBUTION STATEMENT (of this Report) Approved for Public Release; Distribution Unlimited.		
17. DISTRIBUTION STATEMENT (of the abstract entered in Block 20, if different from Report)		
18. SUPPLEMENTARY NOTES		
19. KEY WORDS (Continue on reverse side if necessary and identify by block number) Solid Propellant Rocket Motors Structural Analysis Linear Viscoelasticity Effective Modulus Preliminary Analysis Methods		
20. ABSTRACT (Continue on reverse side if necessary and identify by block number) Software was developed to provide the means to perform a "quick-look" preliminary motor structural analysis within the AFRPL. Preliminary structural analysis equations from the JANNAF Structural Integrity Handbook and Galcit 101, "Fundamental Studies Relating to Systems Analyses of Solid Propellants" were implemented on the HP 9815A programmable calculator as a basis for the software. For analysis of a motor undergoing a thermal transient load, software was written to provide the means to calculate an effective modulus, based		

DD FORM 1473

1 JAN 73

EDITION OF 1 NOV 68 IS OBSOLETE

UNCLASSIFIED

SECURITY CLASSIFICATION OF THIS PAGE (When Data Entered)

UNCLASSIFIED

SECURITY CLASSIFICATION OF THIS PAGE(When Data Entered)

on linear viscoelastic theory, for use in the "quick-look" analysis. Supporting software was also written to provide graphical input of data and to correct any distortions appearing in supplied data. Finally, results from a simple, slow cooldown problem were obtained from a finite element analysis using the TEXGAP 2D computer code to verify the usefulness and accuracy of the "quick-look" analysis and supporting software.

A

UNCLASSIFIED

SECURITY CLASSIFICATION OF THIS PAGE(When Data Entered)

TABLE OF CONTENTS

<u>Section</u>	<u>Page</u>
1. Introduction	5
2. Summary	5
2.1 "Quick-Look" Motor Structural Analysis Software.	5
2.2 Thermal Transient Viscoelastic Response Software	5
2.3 Graphical-Manual Input-Output Facilitating Software	6
2.4 Finite Element Analysis Comparison	6
3. Discussion	6
3.1 "Quick Look" Motor Structural Analysis Software.	6
3.2 Thermal Transient Viscoelastic Response Software	11
3.3 Graphical-Manual Input-Output Facilitating Software	14
3.4 Finite Element Analysis Comparison	15
REFERENCES	21
APPENDICES	
A. Equations Used In the "Quick Look" Structural Analysis Software	22
B. Derivations of Equations Used in the Thermal Transient Viscoelastic Software	35
C. JANNAF Linear Viscoelastic Round Robin Analysis Problem Description and Comparison Results from "Quick Look" Analysis and the TEXGAP Finite Element Analysis	39



Accession For	
NTIS GRA&I	<input checked="" type="checkbox"/>
DTIC TAB	<input type="checkbox"/>
Unannounced	<input type="checkbox"/>
Justification	
By _____	
Distribution/	
Availability Codes	
Dist	Avail and/or Special
A	

LIST OF FIGURES

<u>Figure</u>		<u>Page</u>
1	Temperature History for Thermal Load and Aerodynamic Heating Problems	7
2	Correction Factor - \bar{P}_r	8
3	Correction Factor - \bar{P}_e	9
4	Correction Factor - \bar{P}_θ	9
5	Plot Example	14
6	Time-Temperature Shift Factor vs. Temperature	16
7	Propellant Relaxation Modulus vs. Reduced Time	16
8	Hoop Strain vs. Real Time	17
9	Hoop Stress vs. Real Time	18
10	Bondline Stress vs. Real Time.	18

LIST OF TABLES

<u>Table</u>		<u>Page</u>
I	Comparison of "Quick Look" and TEXGAP Structural Analysis Results (Finite-Length Motor)	19
2	Comparison of "Quick Look" and TEXGAP Structural Analysis Results (Infinite-Length Motor)	20
C1	Geometry, Constraints, and Material Properties	41
C2	Propellant Relaxation Data	42
C3	Additional Data	43
C4	Report of Results for Slow Cooldown	44

I. INTRODUCTION

This report describes the results of an in-house program conducted within the Air Force Rocket Propulsion Laboratory (AFRPL). The objective of the program was to develop a quick-response rocket motor preliminary structural analysis capability within the AFRPL. Task I of the project involved implementation of preliminary structural analysis equations on the HP 9815A calculator. Task II provided the means to calculate an effective modulus input for thermal transient loading based on linear viscoelasticity, and provided for graphical and numerical output utilizing a revision of the linear ramp approximation program used in the original task. Task III provided a graphical and manual data input capability to allow more flexibility and improved accuracy in the overall analysis.

2. SUMMARY

2.1 "Quick-Look" Motor Structural Analysis Software. The preliminary structural analysis methods given in The JANNAF Structural Integrity Handbook (Ref. 1) and the Galcit 101 Technical Report (Ref. 2) were implemented in an interactive, user-oriented program for the HP 9815A calculator. These equations were used to calculate the maximum values of the stresses and strains in the motor bore and case-grain bondline. This type of analysis is usually sufficient to determine whether or not a given grain configuration is feasible and if a more detailed analysis is required. Comparing the preliminary analysis to more complex detailed analyses gives the analyst a reasonable idea of where the results should be falling.

2.2 Thermal Transient Viscoelastic Response Software. Analyses involving a thermal load on a rocket motor require an effective modulus for the propellant at any given time (or temperature). The approach used approximates a time-temperature history by a modified power law that results in a tractable form of the hereditary integral to approximate the stress response. Linear strain and temperature coupling were assumed. The method used to approximate the stress response involved representing the strain (as a function of reduced time) as a series of linear ramp histories. The stress response was calculated for each ramp and combined with each preceding response to obtain the net response required.

2.3 Graphical-Manual Input-Output Facilitating Software. The fact that much of the input data required for the above analyses is available only in graph form established the need for these programs. To complicate matters, many of these graphs are distorted in one way or another (photographs taken at an angle, photocopies from books or folded originals, to name a few); therefore, a capability in the graphical input program was added to correct for these distortions. The other input program allows for manual input of data (i.e., direct from keyboard or calculator). The two output programs allow for storage of data in selected registers and for graphical output in presentable form.

2.4 Finite Element Analysis Comparison. Results from a simple, slow cooldown problem were obtained from a finite element analysis using the TEXGAP 2D computer code and the "Quick-Look" analysis for comparison to verify the usefulness and accuracy of the "Quick-Look" analysis and supporting software.

3. DISCUSSION

3.1 "Quick Look" Motor Structural Analysis Software. The JANNAF Structural Integrity Handbook¹ contains preliminary structural analysis equations that can be very useful for a quick stress-strain analysis of a solid propellant rocket motor. However, use of these equations can involve lengthy hand calculations. To provide a usable "Quick Look" analysis tool, it was decided to implement the equations into a set of software for use on the HP 9815A desk calculator. The equations were checked for consistency and some necessary alterations were made before implementation. The equations were also modified to include variable propellant and material Poisson's ratios.

The equations varied depending on the type of motor configuration and analysis performed; therefore, separate program files were created for each type of analysis. Program files were created for both finite motor correction factor determination and bore stress concentration factor determination for different bore configurations. These program files are used as routines and subroutines in a main program. The exact equations used for the different problems can be found in Appendix A. The aerodynamic heating analysis and the thermal load

analysis use the same equations, except the temperatures used to calculate the shrinkages are different. Specifically, for the thermal load case,

$$\delta = \alpha (T_1 - T_{SF})$$

$$\delta_c = \alpha_c (T_1 - T_{SF})$$

and for the aerodynamic heating case,

$$\delta = \alpha (T - T_1)$$

$$\delta_c = \alpha_c (T_{case} - T_1)$$

where α and α_c are coefficients of linear expansion for the propellant and case, respectively; T_{SF} is the stress-free temperature for the motor; T_1 is the end condition temperature for the thermal load problem and the beginning propellant temperature for the aerodynamic heating problem; T is the final propellant temperature in the aerodynamic heating problem (T is usually taken to be equal to T_1); and T_{case} is the final motor case temperature.

Figure 1 shows the temperature histories for the thermal load and aerodynamic heating problems for temperature input comparison. It can be seen that the value of T_1 is the same for both analyses for a given problem. Although the propellant temperature normally changes somewhat in the real situation, the value T is taken as equal to the value T_1 unless the user specifies a new value for T .

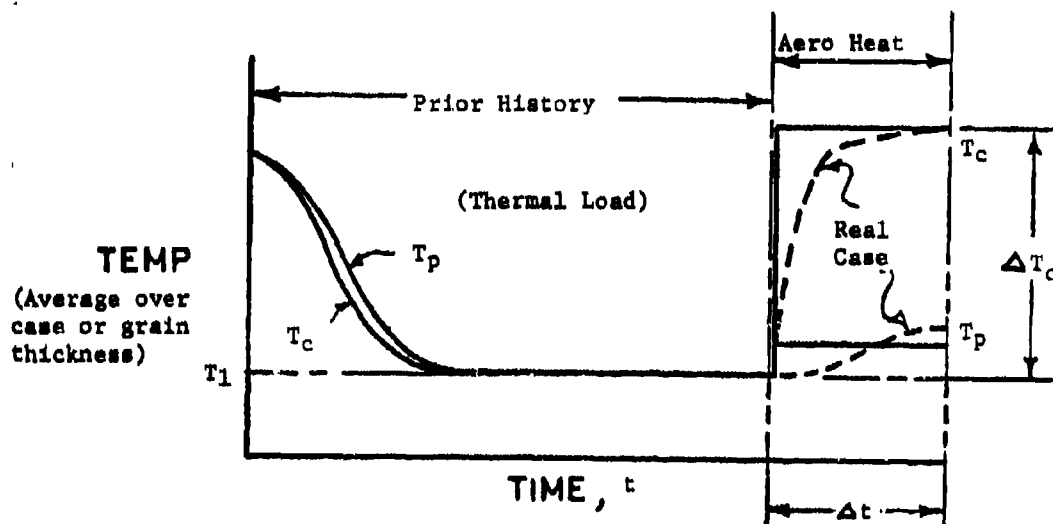


Figure 1. Temperature History for Thermal Load and Aerodynamic Heating Problems

The basic equations are based on the assumption that the rocket motor is of infinite length. This may be a valid assumption in cases where the motor is long and small in diameter, or if the ends are bonded to the case, because the end effects may be negligible. However, for finite-length motors (i.e., stubby and/or free ends), correction factors are needed. These correction factors (\bar{P}_r , \bar{P}_θ , and \bar{P}_z) may be determined from graphs found in The JANNAF Structural Integrity Handbook¹. However, accurate visual interpolation from these graphs is difficult, because the graphs are three dimensional (two independent variables). Using a numerical interpolation method has two distinct advantages. Primarily, fairly good accuracy is achieved--the only error that occurs is due to the fact that the curves cannot be perfectly described by the interpolating functions. The approximations are acceptable for engineering accuracy and all large errors are corrected (Figs. 2 - 4). Second, due to internal storage and numerical interpolation, the user need not look up values, which saves a considerable amount of time. Specifically, the method used is two dimensional Lagrange polynomial interpolation that approximates the surfaces created by the graphs with a polynomial of two independent variables. This method requires data from the graphs to be set up in an internal matrix. Enough data had to be used to adequately represent the graph (usually a 7 x 7 matrix was sufficient). This data required a significant amount of memory space; therefore, each graph used a separate data file on tape. The software manipulates the data files in order to conserve memory space.

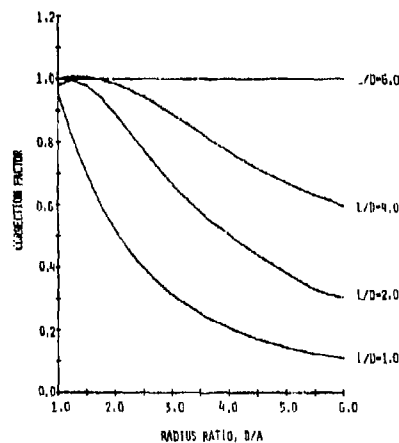


Figure 2. Correction Factor - \bar{P}_r

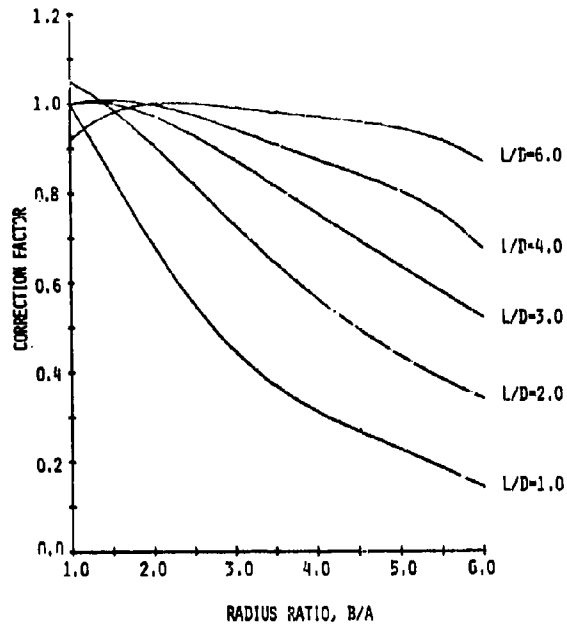


Figure 3. Correction Factor - \bar{P}_e

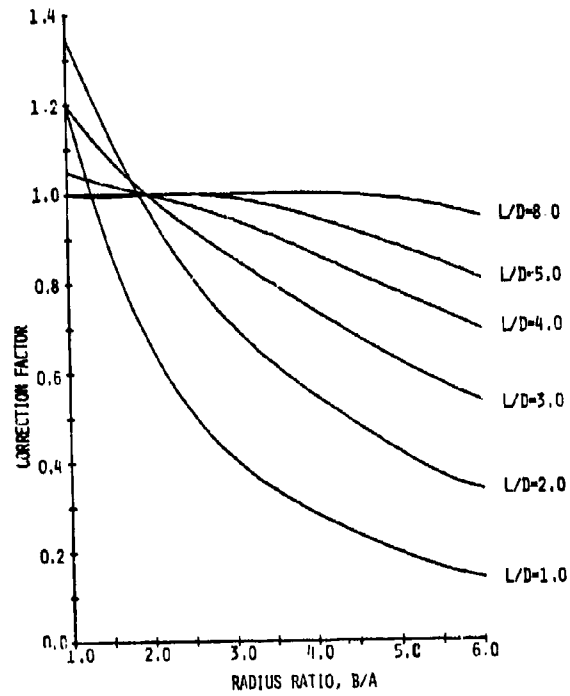


Figure 4. Correction Factor - \bar{P}_θ

The basic equations are set up for motors with circular ports, and do not include stress and strain concentrations occurring in the tips of slotted ports. To incorporate these effects, equations were implemented to calculate the stress-strain concentration factors for varying slot tip configurations. The equations used were originally derived from elastic models undergoing infinitesimal strains. However, in regions of high stress concentration in viscoelastic material, large deformations can be expected. These large deformations tend to reduce the stress concentration, because the material deforms into a more ideal structural shape. Therefore, the concentration factors obtained tend to be on the conservative side.

The acceleration and vibration analyses were not implemented at the time of this writing. The main program lists these analyses as choices and the file exists, but the programs are still under development. The thermal load, aerodynamic heating, and ignition pressure analyses were implemented first because of similarities, and due to the fact that these analyses were required most often. The acceleration and vibration analyses involve dynamic loads that require a different procedure.

After the software was tested for consistency with sample problems, it was decided to allow for user input of the Poisson's ratio for both case and propellant. The equations found in The JANNAF Structural Integrity Handbook¹ assumed a Poisson's ratio of 0.50 for the propellant and 0.33 for the case. Derivations were not included; therefore, another source was required. The Galcit 101 Technical Report² contains equations with variable Poisson's ratios. These equations were used to obtain equations of the form found in The JANNAF Structural Integrity Handbook¹.

The capabilities of the "Quick Look" Structural Analysis software are outlined below:

a. Stress-Strain Analysis Selection. Any or all of the following analyses may be selected:

- Thermal Soak
- Aerodynamic Heating

Acceleration Effects - under development

Ignition Pressure

Vibration Effects - under development

b. Various Simple Grain Configurations. The user may select from the following configurations:

Circular Port

Slotted Port

The following slot tip configurations may be selected: semicircular, elliptical, or filed flat-bottomed.

c. Finite-Length Correction. For values of a/b , correction factors are found by Lagrange polynomial interpolation of internal graphs. If no finite-length correction is necessary the correction factors are assigned to the value of one (1).

d. Superposition. After all the analyses have been performed, the final program file sums all corresponding stresses and strains to obtain a net result.

3.2 Thermal Transient Viscoelastic Response Software. A stress-strain analysis of a solid propellant rocket motor undergoing a thermal load requires that an effective modulus of elasticity be known for any given time (or temperature). To obtain an effective modulus for a propellant, some knowledge is required of the viscoelastic processes that occur in the propellant under a thermal load. One of the complexities involved in the analysis of a viscoelastic material is the change of viscosity with change of temperature. With a change in temperature of a material with linear viscoelastic properties, a time shift occurs in the response. To obtain a continuous net response, the individual curves (plotted on log-log coordinates) are shifted so they fall on a single master curve. The time-temperature shift factors are determined at specific temperatures by applying a step load to a specimen at a constant temperature. The response is then recorded and plotted on log-log coordinates. This process is repeated at the specified temperatures to obtain each response. The time-temperature shift factors can then be determined visually or by numerical methods. A modified power law was used to represent the time-temperature

shift factors as a function of temperature. The "reduced time" is then determined using the "Moreland-Lee Hypothesis," the representation of the time-temperature shift factors, and the temperature history. The "Moreland-Lee Hypothesis" states that for a nonconstant temperature history, the reduced time can be represented by an integral,

$$\xi = \int_{-\infty}^t \frac{dt}{a_T}$$

Appendix B contains an analytical equation for the reduced time that was derived for use in the software along with the derivation.

Using the assumption the strain and temperature are linearly coupled, the strain history in terms of reduced time can be computed. A method was then required to determine the stress response utilizing the hereditary integral. Polynomial representation and piecewise linear ramp approximation were the approaches considered. A polynomial representation of the strain history would have allowed a direct solution of the stress response. However, the representation was too complex and inaccurate and, therefore, was not used. Representation of the strain history by piecewise linear ramps proved viable and accurate and was, consequently, the method used. Basically, the method involves breaking up the strain history into a series of linear ramp histories. The stress response for each ramp is computed and added to each preceding response in order to obtain the approximate net stress response. The output values of stress are calculated at offset values of reduced time [i.e., $\xi_s = \xi_{t-1} + k_\sigma (\xi_t - \xi_{t-1})$ where $0 \leq k_\sigma \leq 1$], which results in a more accurate representation of the stress response. k_σ is found by trial and error (a typical value for k_σ is .833), and should be fairly non-sensitive if a large number of ramps are used.

To evaluate the hereditary integral, the relaxation modulus must be known for any given reduced time. The relaxation modulus data is normally given as the net response obtained from the propellant relaxation tests. A modified

power law fit was used once again to represent the data in a form the calculator could easily handle. If the temperature normalized form of the relaxation modulus data is given [i.e., $E_r = \left(\frac{T}{T_0}\right) E_r$], then the computed stresses must be corrected by multiplying the stress values by corresponding factors of $\left(\frac{T}{T_0}\right)$.

From the values of stress and corresponding values of strain, an effective modulus (σ/ϵ) may be computed at each output point. Values of real time can also be computed by using the same equations that were used to compute reduced time.

The capabilities of the thermal transient viscoelastic response software are outlined below:

- a. Representation of Relaxation Modulus Data. Modified power law fit by a least squares iterative method.
- b. Representation of Time-Temperature Shift Factor Data. Modified power law fit through three points.
- c. Representation of Temperature Rate. Modified power law fit through three points. Exact representation of constant temperature rate (linear temperature history).
- d. Plot or Storage for Ramps Approximation. Plot or storage of strain history (in terms of reduced time). Plot nontime also allows visual representation of ramp approximation for use as a check.
- e. Allows for Correction of Stress.
- f. Choice of Plot or Table of Data. Allows choice of parameters to be plotted or printed on hard copy. Data is not stored. Parameters are as follows:
 - Real Time, t
 - Reduced Time, ξ
 - Strain, ϵ
 - Stress, σ
 - Effective Modulus, $E\left(\frac{\sigma}{\epsilon}\right)$

3.3 Graphical-Manual Input-Output Facilitating Software. Data needed for analysis may come in several different forms that require special attention. Data in tabulated form usually can be handled easily by direct input. However, data in graphical form can be difficult to use, particularly if the graph contains distortions due to photocopy errors, etc. The HP 9862A plotter has a unique feature that allows the user to digitize graphs. Basically, the user places the plotter in the digitizer mode, moves the pen (pointer) over the point of interest, and then exits the digitizer mode. The coordinates of the point are entered into the calculator automatically. However, the digitizer assumes the graph is undistorted. Therefore, for distorted graphs, corrections need to be made. The method used to correct distorted graphs was Lagrange shape functions (Ref. 3). This technique maps an undistorted grid defined by the user into the distorted grid, thereby creating an internal distorted grid, which when digitized, will produce correct data. This data may then be replotted in a presentable form using the plotting routine (Fig. 5), or stored in user selected registers using the data manipulation routine. The plotting routine utilizes a cubic spline subroutine (Ref. 4) to accurately fit sparse data. The plotting routine will accept data from either the manual input program or the digitizing program.

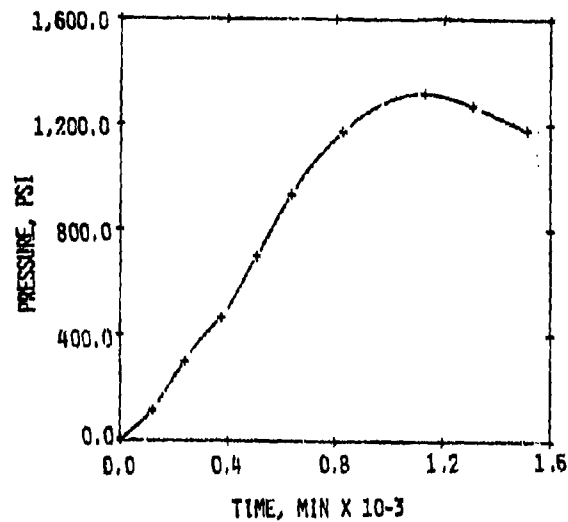


Figure 5. Plot Example.

The capabilities of these programs follow.

a. Data Input

(1) Manual Input. Direct input of data into calculator through keyboard. Used when tabulated numerical data is available.

(2) Digitize/Correct. Input of data by way of the HP 9862A Plotter/Digitizer. Used when data is in graph form only. Distorted graphs (i.e., perspective-linear and warped-curved distortions) are corrected by using a technique that utilizes Lagrange shape functions.

b. Data Output

(1) Allows user to define the memory area in which to store the inputted data for use elsewhere. Data may be stored on tape.

(2) Plot. Allows user to plot data. Allows for any size graph (to plotter limits), axis headings, and graph titles.

3.4 Finite Element Analysis Comparison

To verify the validity and usefulness of the "Quick Look" structural analysis software, a simple, slow cooldown problem was run on this software and on the TEXGAP 2D finite element computer code (Ref. 5). The problem description and results can be found in Appendix C.

Several plots were made to show the accuracy of the representations of the time-temperature shift factors and the relaxation modulus rate (Figs. 6 and 7). Figure 6 also shows the control data points. These points were the data used in the program to represent the time-temperature shift factors. As can be seen, these points lie on the curve, and the mid and final points are true data points. The first point is not an actual data point; it was chosen so the resulting curve would best represent the actual data.

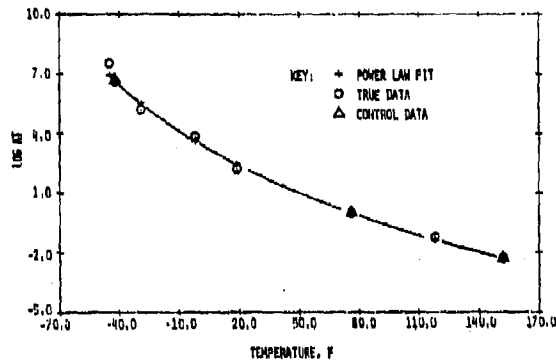


Figure 6. Time-Temperature Shift Factor vs Temperature.

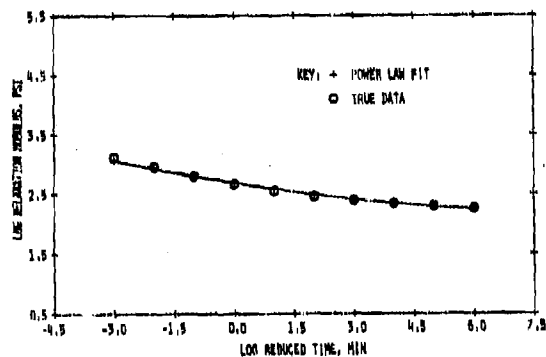


Figure 7. Propellant Relaxation Modulus vs Reduced Time.

Plots were also made of the final results from the "Quick Look" structural analysis (Figs. 8 - 10). These results in numerical form were compared to the results found with the TEXGAP 2D code. The "Quick Look" structural analysis produces stresses and strains theoretically located at the bore surface and bondline in the axial midplane of the motor, while the TEXGAP 2D code produces stresses and strains throughout the motor case and grain that is defined by an element grid. Therefore, the values obtained from the TEXGAP analysis were taken from elements whose sides were located on the axial midplane of the motor. The average percent difference (using the "Quick Look" structural analysis results as the base values) for the axisymmetric problem was around 4 percent to 6 percent (Table 1). The difference in the results may be attributed to many reasons. Namely, these analyses are determined by two totally different approaches. The "Quick Look" structural analysis equations are a

direct method for obtaining preliminary results. The TEXGAP 2D code is an analysis designed to give the analyst a detailed view of the stress state in a motor undergoing a given load, but it is not necessarily going to give highly accurate results at specific points within the motor, since the accuracy depends on the fineness of the finite element grid. The "Quick Look" structural analysis gives theoretically exact results, but errors can result in the determination of the correction factors. As mentioned previously, the correction factors are determined through an interpolation technique and are, therefore, approximate. Because of this uncertainty in the determination of the correction factors, a second analysis was done using the same motor parameters as before, but with an infinite length. The average percent difference was around 1.3 percent to 5 percent (Table 2). The largest percent difference occurred in the values of the hoop strain (5 percent). These percent differences are within acceptable engineering standards.

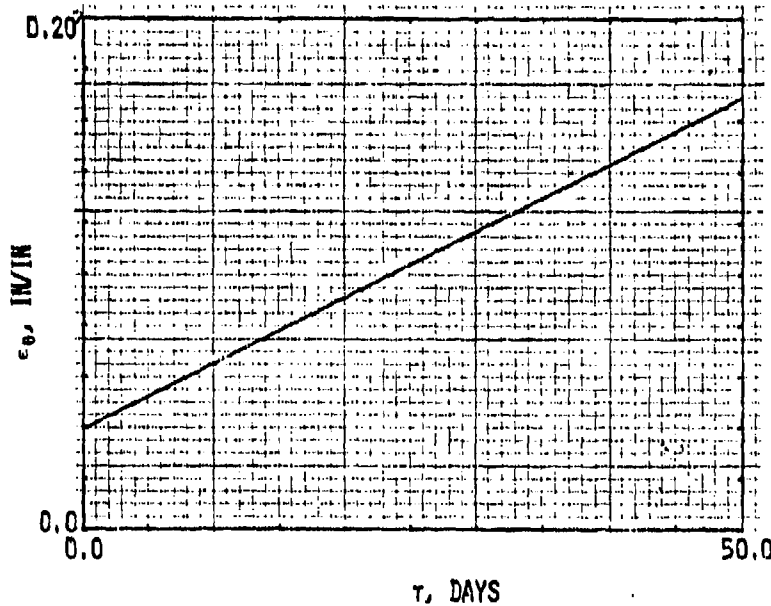


Figure 8. Hoop Strain vs Real Time

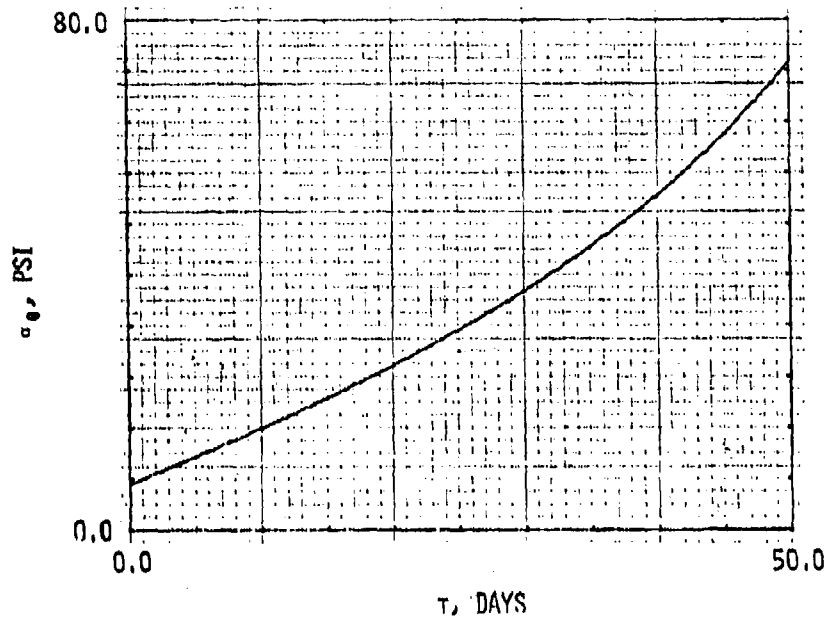


Figure 9. Hoop Stress vs. Real Time

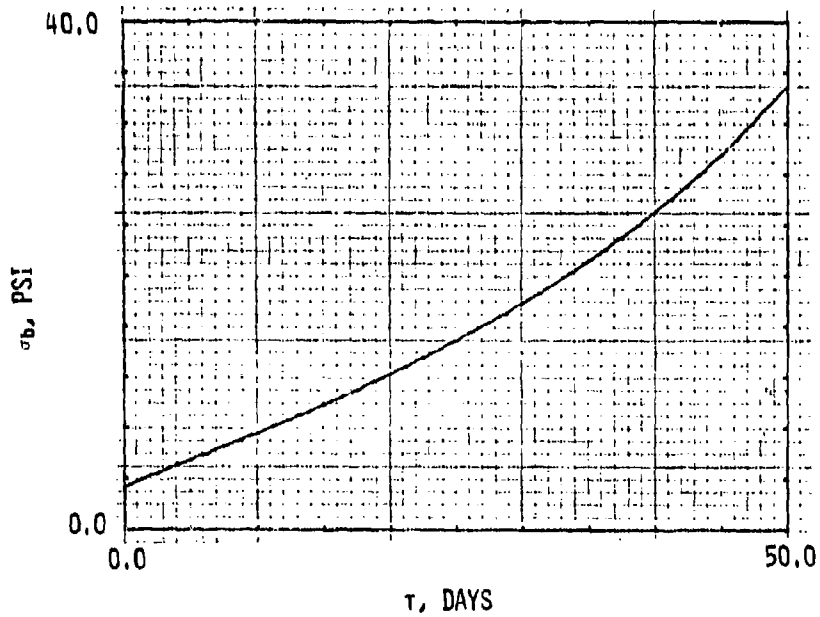


Figure 10. Bondline Stress vs Real Time.

Table 1. Comparison of "Quick Look" and TEXGAP Structural Analysis Results (Finite-Length Motor).

Temp	Quick-Look Results	TEXGAP Results	% Diff	Temp	Quick-Look Results	TEXGAP Results	% Diff		
80°	σ_b	3.33	3.20	-3.9	30°	σ_b	14.94	14.40	-3.6
	σ_θ	6.98	6.60	-5.4		σ_θ	31.33	29.60	-5.5
	ϵ_θ	.0390	.0373	-4.4		ϵ_θ	.1038	.0995	-4.1
70°	σ_b	5.47	5.26	-3.8	20°	σ_b	17.87	17.20	-3.8
	σ_θ	11.64	10.9	-6.4		σ_θ	37.49	35.5	-5.3
	ϵ_θ	.0519	.0497	-4.2		ϵ_θ	.1168	.1120	-4.1
60°	σ_b	7.59	7.31	-3.7	10°	σ_b	21.19	20.40	-3.7
	σ_θ	15.93	15.1	-5.2		σ_θ	44.45	42.10	-5.3
	ϵ_θ	.0649	.0622	-4.2		ϵ_θ	.1298	.1240	-4.5
50°	σ_b	9.85	9.48	-3.8	0°	σ_b	25.00	24.10	-3.6
	σ_θ	20.65	19.6	-5.1		σ_θ	52.43	49.60	-5.4
	ϵ_θ	.0779	.0746	-4.2		ϵ_θ	.1428	.1370	-4.1
40°	σ_b	12.27	11.80	-3.8	-10°	σ_b	29.46	28.30	-3.9
	σ_θ	25.75	24.40	-5.2		σ_θ	61.79	58.50	-5.3
	ϵ_θ	.0909	.0870	-4.3		ϵ_θ	.1558	.1490	-4.4

% Difference

Term	Average	Std Dev
σ_b	-3.76	.11
σ_θ	-5.41	.37
ϵ_θ	-4.25	.14

STATISTICAL SUMMARY:

Table 2. Comparison of "Quick Look" and TEXGAP Structural Analysis Results (Infinite-Length Motor).

Temp	Quick-Look Results	TEXGAP Results	% Diff	Temp	Quick-Look Results	TEXGAP Results	% Diff	
80°	σ_b	3.39	1.50	30°	σ_b	15.23	15.30	
	σ_θ	7.12	2.45		σ_θ	31.9	31.2	-2.24
	ϵ_θ	.0409	4.87		ϵ_θ	.1090	.1040	4.81
70°	σ_b	5.58	1.45	20°	σ_b	18.23	18.00	
	σ_θ	11.7	2.63		σ_θ	38.2	37.4	2.14
	ϵ_θ	.0545	5.01		ϵ_θ	.1226	.1170	4.79
60°	σ_b	7.75	1.57	10°	σ_b	21.62	21.30	
	σ_θ	16.2	1.89		σ_θ	4.53	44.3	2.26
	ϵ_θ	.0681	4.93		ϵ_θ	.1362	.1300	4.77
50°	σ_b	10.04	1.41	0°	σ_b	25.50	25.10	
	σ_θ	21.1	2.43		σ_θ	53.5	52.3	2.29
	ϵ_θ	.0817	4.90		ϵ_θ	.1498	.1430	4.76
40°	σ_b	12.52	1.79	-10°	σ_b	30.05	29.6	
	σ_θ	26.3	2.33		σ_θ	63.0	61.6	2.27
	ϵ_θ	.0953	4.88		ϵ_θ	.1634	.1560	4.74

20

% Difference

Term	Average	Std Dev
σ_b	1.32	.64
σ_θ	2.29	.20
ϵ_θ	4.85	.09

STATISTICAL SUMMARY:

REFERENCES

1. The JANNAF Structural Handbook, Chemical Propulsion Information Agency, Publication No. 230, September 1972.
2. Williams, M. L., P. J. Blatz, and R. A. Schapery, "Fundamental Studies Relating to Systems Analysis of Solid Propellants," Gugenheim Aeronautical Laboratory, California Institute of Technology, Pasadena, CA. Final Report - Galcit 101, Thiokol Subcontract No. RS-69752, February 1961.
3. Francis, E. C., et al, "Case Liner Bond Analysis," United Technology Center, Sunnyvale, CA, AFRPL-TR-74-23, June 1974.
4. Gerald, C. F., "Applied Numerical Analysis," 2nd ed, California Polytechnic State University, San Luis Obispo, CA, May 1980.
5. Becker, E. B., and R. S. Dunham, "TEXGAP 2D Documentation," Thiokol Corporation, Huntsville, AL, AFRPL-TR-78-86, February 1979.

APPENDIX A

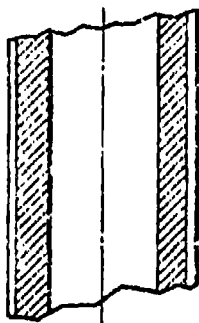
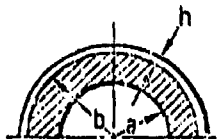
Equations Used in the "Quick Look" Structural

Analysis Software

Thermal Load

PROBLEM DESCRIPTION

I DIFFERENTIAL SHRINKAGE
OF LONG CIRCULAR-PORT,
CASE-BONDED GRAINS



$$\sigma_b = E\delta \left\{ \frac{(1 + \nu_c) \left(\frac{\delta_c}{b}\right) - (1 + \nu)}{(1 + \nu) \left[(1 - 2\nu) + \left(\frac{a}{b}\right)^2 \right] + (1 - \nu_c^2) \frac{bE}{hE_c}} \right\}$$

$$\sigma_\theta = \frac{2\sigma_b}{1 - \left(\frac{a}{b}\right)^2}$$

$$\sigma_z = (\sigma_\theta)\nu - E\delta$$

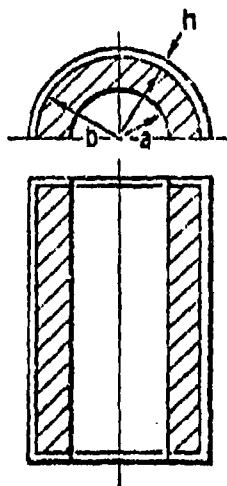
$$\epsilon_\theta = \frac{\sigma_\theta}{E} (1 - \nu^2) + \delta \nu$$

$$\epsilon_z = -\delta$$

Thermal Load

PROBLEM DESCRIPTION

□ DIFFERENTIAL SHRINKAGE OF
FINITE - LENGTH CYLINDER -
BONDED ENDS

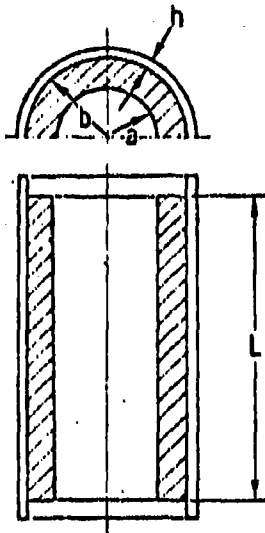


Same Equations as for Problem I

Thermal Load

PROBLEM DESCRIPTION

□ DIFFERENTIAL SHRINKAGE OF
FINITE-LENGTH, CIRCULAR-
PORT CASE-BONDED
GRAINS-ENDS FREE



- IF ENDS ARE DOME-SHAPED,
INCLUDE 1/2 OF DOME
HEIGHT IN L

$$\sigma'_b = \sigma_b \times F_r$$

$$\sigma'_\theta = \frac{2\sigma'_b}{1 - \left(\frac{b}{r}\right)^2}$$

$$\sigma'_z = (\sigma'_\theta)\nu - E\delta$$

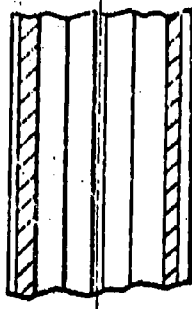
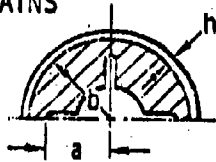
$$\epsilon'_\theta = F_c \left[\frac{\sigma_\theta}{E} (1 - \nu^2) + \delta\nu \right]$$

$$\epsilon'_z = -\delta$$

Thermal Load

PROBLEM DESCRIPTION

IV DIFFERENTIAL SHRINKAGE OF LONG SLOTTED-PORT, CASE-BONDED GRAINS OR END-BONDED, FINITE-LENGTH GRAINS



If $\frac{a}{b} \leq 0.5$, $\sigma_b = \sigma_b$.

If $\frac{a}{b} > 0.5$, $\sigma_b = \sigma_b$

but with an equivalent $\left(\frac{a}{b}\right)^2$

$$\left(\frac{a}{b}\right)_E^2 = \left(\frac{a}{b}\right)^2 - 0.2 \left[\left(\frac{a}{b}\right)^2 - \left(\frac{a}{b}\right)_A^2 \right]$$

where subscript A denotes calculation of $\left(\frac{a}{b}\right)^2$ using a radius "a" of a circular port of equivalent cross sectional area to the slotted port.

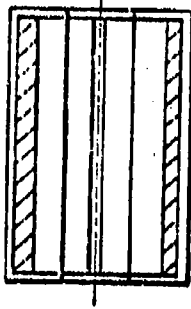
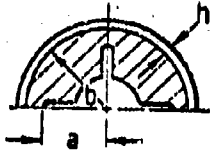
$$\sigma_T = H\sigma_b$$

where H is a stress concentration factor for slotted ports.

Thermal Load

PROBLEM DESCRIPTION

DIFFERENTIAL SHRINKAGE OF
LONG SLOTTED-POR, CASE-
BONDED GRAINS OR END-
BONDED, FINITE-LENGTH
GRAINS



$$\sigma_z = (\sigma_T)\nu - E\delta$$

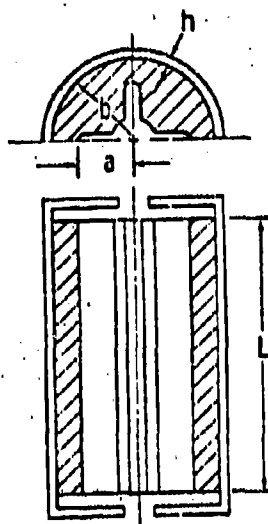
$$\epsilon_\theta = \frac{\sigma_T}{E}(1 - \nu^2) + \delta\nu$$

$$\epsilon_z = -\delta$$

Thermal Load

PROBLEM DESCRIPTION

DIFFERENTIAL SHRINKAGE OF
FINITE-LENGTH, CASE-BONDED
SLOTTED-PORT,
GRAINS-ENDS FREE



• IF ENDS ARE DOME-SHAPED,
INCLUDE 1/2 OF DOME
HEIGHTS IN L

$$\sigma_T = H\sigma_b$$

$$\sigma_z = (\sigma_c^0)\nu - E\delta$$

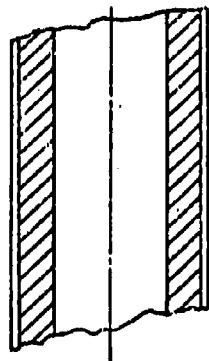
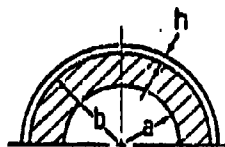
$$\epsilon_\theta = \bar{P}_c \left[\frac{\sigma_T}{E} (1 - \nu^2) + \delta\nu \right]$$

$$\epsilon_z = -\delta$$

Pressure Load

PROBLEM DESCRIPTION

I LONG CIRCULAR-PORT GRAIN WITH INTERNAL PRESSURE. LOADING



$$\sigma_b = \frac{-P \left(\frac{a}{b}\right)^2}{\left(\frac{a}{b}\right)^2 + (1 - 2\nu)} + \frac{(1 - \nu_c^2) b E}{(1 + \nu) h E_c} \left[1 - \left(\frac{a}{b}\right)^2 \right]$$

$$\sigma_\theta = \frac{P \left[1 + \left(\frac{a}{b}\right)^2 \right] + 2\sigma_b}{1 - \left(\frac{a}{b}\right)^2}$$

$$\sigma_z = \frac{\left[P \left(\frac{a}{b}\right)^2 + \sigma_b \right] 2\nu}{1 - \left(\frac{a}{b}\right)^2}$$

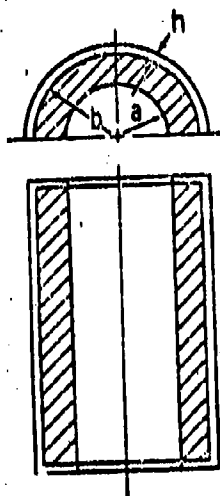
$$\epsilon_\theta = \frac{(1 + \nu)(P + \sigma_b)}{\left[1 - \left(\frac{a}{b}\right)^2 \right] E}$$

$$\epsilon_z = \frac{1}{E} [\sigma_z - \nu (\sigma_\theta - P)]$$

Pressure Load

PROBLEM DESCRIPTION

- FINITE-LENGTH,
CIRCULAR-PORT GRAIN
WITH INTERNAL PRESSURE
LOADING-ENDS BONDED

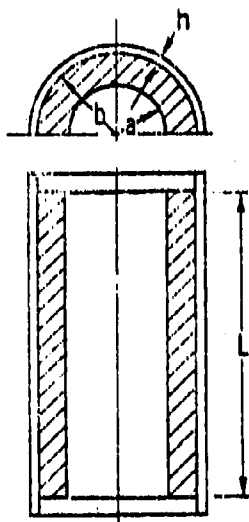


Same equations as for Problem I

Pressure Load

PROBLEM DESCRIPTION

III FINITE-LENGTH, CIRCULAR-PORT GRAIN WITH INTERNAL PRESSURE LOADING-ENDS FREE



$$\sigma'_b = \sigma_b \times F_T - (1 - F_T)P$$

$$\sigma'_\theta = \sigma_\theta \times F_\theta - (1 - F_\theta)P$$

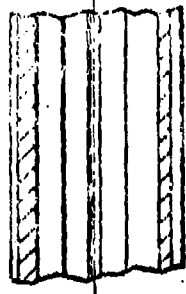
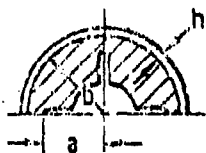
$$\epsilon'_\theta = \epsilon_\theta \times F_c$$

• IF ENDS ARE DOME-SHAPED, ADD 1/2 DOME HEIGHTS TO L

Pressure Load

PROBLEM DESCRIPTION

IV LONG SLOTTED-PORT GRAIN WITH INTERNAL PRESSURE LOADING OR FINITE-LENGTH GRAIN WITH ENDS BONDED



If $\frac{a}{b} \leq 0.5$, $\sigma_b = \sigma_b$.

If $\frac{a}{b} > 0.5$, $\sigma_b = \sigma_b$

but with an equivalent $\left(\frac{a}{b}\right)^2$

$$\left(\frac{a}{b}\right)_E^2 = \left(\frac{a}{b}\right)^2 - 0.2 \left[\left(\frac{a}{b}\right)^2 - \left(\frac{a}{b}\right)_A^2 \right]$$

where subscript A denotes calculation of $\left(\frac{a}{b}\right)^2$ using a radius "a" of a circular port of equivalent cross sectional area to the slotted port.

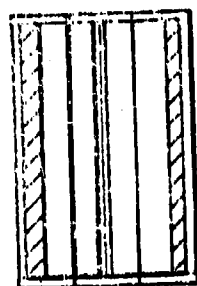
$$\sigma_T = H(P + \sigma_b) - P$$

where H is a stress concentration factor for the slotted ports.

Pressure Load

PROBLEM DESCRIPTION

LONG SLOTTED-PORT GRAIN
WITH INTERNAL PRESSURE
LOADING OR FINITE-LENGTH
GRAIN WITH ENDS BONDED



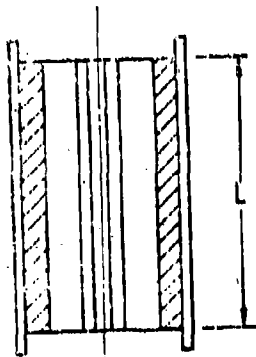
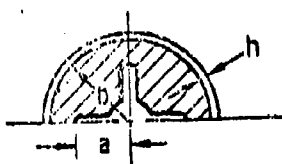
$$\sigma_z = Hv(P + \sigma_b) - P$$

$$\epsilon_T = \frac{H}{R}(P + \sigma_b)(1 - \nu^2)$$

Pressure Load

PROBLEM DESCRIPTION

V FINITE-LENGTH, SLOTTED-PORT
GRAIN WITH INTERNAL
PRESSURE LOADING-ENDS
FREE



• IF ENDS ARE DOME-SHAPED
ADD 1/2 OF DOME HEIGHTS
TO L.

$$\sigma_T^c = H(P + \sigma_b^c) - P$$

$$\sigma_Z^c = Hv(P + \sigma_b^c) - P$$

$$\sigma_T^c = \bar{P}_e \left[\frac{H}{B} (P + \sigma_b) (1 - \nu^2) \right]$$

APPENDIX B

**Derivations of Equations Used in the
Thermal Transient Viscoelastic Software**

$$\sigma = \int_0^{\xi'} E_T (\xi - \xi') \frac{dE}{d\xi} d\xi'$$

$$E_T = \left(\frac{T}{T_0}\right) [\hat{E}_1(\xi^n) + \hat{E}_\infty]$$

and

$$\epsilon = \epsilon_0 + k_\epsilon (T - T_1)$$

$$k_\epsilon = (k_{\epsilon_V} - \alpha)$$

$$\sigma = \int_0^{\xi'} \left(\frac{T}{T_0}\right) \hat{E}_1 [\xi^n - (\xi')^n] \frac{dE}{d\xi'} d\xi' + \left(\frac{T}{T_0}\right) \hat{E}_\infty \epsilon \Big|_0^{\xi'}$$

assume that the $\left(\frac{T}{T_0}\right)$ term can be taken outside the integral;

then

$$\sigma = \left(\frac{T}{T_0}\right) \left[\int_0^{\xi'} \hat{E}_1 [\xi^n - (\xi')^n] \frac{dE}{d\xi'} d\xi' + \hat{E}_\infty \epsilon \Big|_0^{\xi'} \right]$$

By definition.

$$\xi = \int_0^t \frac{d\tau}{a_T} \quad \xi' = \int_0^{\tau} \frac{d\tau}{a_T}$$

$$\text{let } a_T = \omega^{-m} \text{ where } \omega = \left(\frac{T + C}{T_0 + C} \right)$$

$$d\xi = \frac{dt}{a_T} = \frac{dT}{a_T} \frac{dt}{dT} = \frac{1}{R_T} \frac{dT}{a_T}$$

$$\frac{d\omega}{dT} = \frac{1}{T_0 + C}$$

$$dT = (T_0 + C) d\omega$$

$$\text{therefore, } d\xi = \frac{(T_0 + C) \omega^m d\omega}{R_T}$$

$$\text{Let } R_T = \frac{R\omega^P}{1-P}$$

$$\text{then, } d\xi = \frac{(1-P)(T_0 + C)\omega^{m-P}}{R} d\omega$$

$$\xi = \frac{(1-P)(T_0 + C)}{R} \int_{\omega_1}^{\omega} \omega^{m-P} d\omega$$

$$\xi = \frac{(1-P)(T_0 + C)}{R(1-P+m)} (\omega^{(1-P+m)} - \omega_1^{(1-P+m)})$$

$$\frac{d\omega}{dt} \frac{dt}{dT} = \frac{1}{T_0 + C}$$

$$\frac{d\omega}{dt} = \frac{R_T}{T_0 + C}$$

$$dt = \frac{(T_0 + C)}{R_T} d\omega$$

$$dt = \frac{(1-P)(T_0 + C)}{R_T} \omega^{-P} d\omega$$

$$t = \frac{(1 - P)(T_o + C)}{R} \int_{\omega_1}^{\omega} \omega^{-P} d\omega$$

$$t = \frac{(T_o + C)}{R} (\omega^{1-P} - \omega_1^{1-P})$$

$$\xi = \frac{(1 - P)(T_o + C)}{R(1 - P + m)} (\omega^{(1-P+m)} - \omega_1^{(1-P+m)})$$

$$\omega^{(1-P+m)} = \frac{R\xi(1 - P + m)}{(1 - P)(T_o + C)} + \omega_1^{(1-P+m)}$$

$$\omega = \left[\frac{R\xi(1 - P + m)}{(1 - P)(T_o + C)} + \omega_1^{(1-P+m)} \right]^{\frac{1}{(1-P+m)}}$$

$$t = \left\{ \left[\frac{R(1 - P + m)}{(1 - P)(T_o + C)} \xi + \omega_1^{(1-P+m)} \right]^{\frac{(1-P)}{(1-P+m)}} - \omega_1^{(1-P+m)} \right\} \frac{(T_o + C)}{R}$$

APPENDIX C

JANNAF linear viscoelastic Round Robin analysis problem description and comparison results from the "Quick Look" analysis and the TEXGAP finite element analysis.

The description contains two problems. Problem 1, only the slow cooldown problem was analyzed; therefore, references to Problem 2 may be ignored.

JANNAF STRUCTURES AND MECHANICAL
BEHAVIOR SUBCOMMITTEE (S&MBS)

JANNAF EXPERIMENTAL AND ANALYTICAL STRUCTURAL METHODS PANEL
LINEAR VISCOELASTIC ROUND ROBIN

I. BACKGROUND

A. Introduction

Problem: Several methods of analyzing solid propellant motor stresses and strains based on linear viscoelastic theory are in use by propulsion contractors and government agencies. These include "quasi-elastic" methods (in which elastic analyses by finite element codes are used together with certain mathematical procedures to provide viscoelastic response) and "linear viscoelastic" computer codes. The degree to which these methods yield the same results when applied to the same problem is unknown.

B. Objective

The objective of this "round robin" analysis is to collect results from different analysts, using various techniques, on the same quasi-static linear viscoelastic problem. These results will be tabulated and reported to the JANNAF S&MBS. The overall goal is to determine how consistent the various analytical procedures are - i.e., do they all yield similar results?

C. Ground Rules

Confidentiality of the source will be maintained in all reporting of results. The source of individual analysis results will be known only to the reviewers and will be used only for follow-up questions and for recognition of participation. Participants may elect to analyze either one (or both) of the two problems posed below. Each participant will be provided a copy of the report. By stating intent to participate, each participant agrees to carry out the analysis according to the problem statement, to provide a report of the results, and to respond to subsequent reasonable queries for additional information. The voluntary nature of this participation is clearly recognized, however.

II. PROBLEM DESCRIPTION

A. This round robin analysis consists of two motor analysis problems:

Problem No. 1. A "slow" cooldown (slow enough to maintain thermal equilibrium throughout the propellant grain).

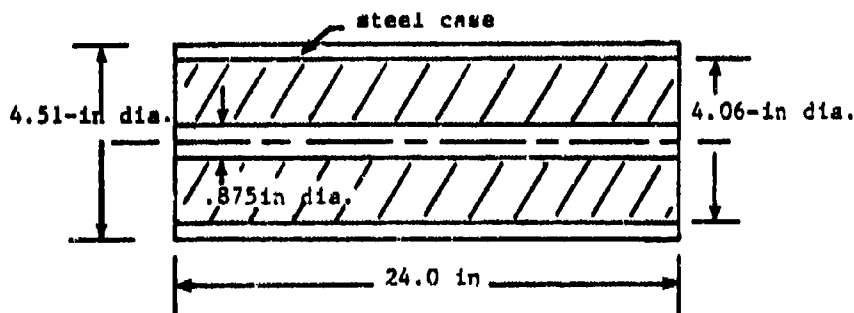
Problem No. 2. A "rapid" cooldown problem, in which thermal equilibrium cannot be assumed.

B. Analysis approaches may include your normal techniques or other methods. The propellant shall be treated as a "Thermorheologically simple material." Other simplifications to propellant material behavior may be applied as well. All assumptions and simplifications (e.g., numerical integration techniques) shall be reported.

C. The problem details are given in Tables 1 through 4. Tables 1 through 3 provide data that are common to both problems. Table 4 gives the temperature-time "histories" for Problems No. 1 and 2, respectively.

D. The results shall be reported on the "Report of Results" forms (Tables 4 and 5). A narrative report is also encouraged.

TABLE I. Geometry, Constraints and Material Properties.



Steel Case Properties:

$$E = 3 \times 10^7 \text{ psi}$$

$$\nu = 0.31$$

$$\alpha = 6 \times 10^{-6} \text{ in/in/}^\circ\text{F}$$

Propellant Properties:

E (see Propellant Relaxation Data) (Table 2)

$$\nu = 0.499$$

$$\alpha = 5 \times 10^{-5} \text{ in/in/}^\circ\text{F}$$

Motor Stress Free Temperature: 110°F

TABLE 2. Propellant Relaxation Data.

Propellant Stress Relaxation Modulus

Reduced time, min	E_{rel} , psi
10^{-3}	1,300
10^{-2}	900
10^{-1}	630
10^0	460
10^1	355
10^2	290
10^3	250
10^4	220
10^5	200
10^6	180
10^7	168
10^8	150

Time-Temperature Shift Factor

Temperature, °F	Log A _T
-45	7.52
-42	6.60
-29	5.19
-2	3.84
19	2.20
76	0.00
118	-1.23
152	-2.30

TABLE 3. Additional Data.

Steel thermal properties:

- $\rho = 0.282 \text{ lb/in}^3$
- $c_p = 0.127 \text{ BTU/ft-F}$
- $k = 266 \text{ BTU/hr ft}^2\text{-F}$

Propellant thermal properties:

- $\rho = 0.0636 \text{ lb/in}^3$
- $c_p = 0.298 \text{ BTU/ft-F}$
- $k = 0.275 \text{ BTU/hr ft}^2\text{-F}$

TABLE 4. Report of Results for Slow Cooldown

Problem No. 1. Slow Cooldown (2°F/day).

Elapsed time, days	Temperature, °F	Hoop strain ϵ_{θ} , in/in	Hoop Stress σ_{θ} , psi	Bond stress σ_b , psi
0	80			
5	70			
10	60			
15	50			
20	40			
25	30			
30	20			
35	10			
40	0			
45	-10			
50	-20			